Chemico-Biological Interactions 345 (2021) 109514

Contents lists available at ScienceDirect

Chemico-Biological Interactions

journal homepage: www.elsevier.com/locate/chembioint

Research paper

Structural design, synthesis and anti-*Trypanosoma cruzi* profile of the second generation of 4-thiazolidinones chlorine derivatives

Gevanio Bezerra de Oliveira Filho [a], Marcos Veríssimo de Oliveira Cardoso [b], Aline Caroline da Silva Santos [c], Thiago André Ramos dos Santos [c], Ana Catarina Cristovão-Silva [c], Laura González Rubio [a], Luiz da Silva Maia Neto [a], Paulo Gaio Leite [d], Fabiana Simão Machado [d], Luiz Carlos Alves [e,f], Fabio André Brayner [e,f], Valéria Rêgo Alves Pereira [c], Ana Cristina Lima Leite [a,*]

[a] Department of Pharmaceutical Sciences, Health Sciences Center, Federal University of Pernambuco, 50740-520, Recife, PE, Brazil
[b] Laboratory of Prospecting Bioactive Molecules, University of Pernambuco, 56328-903, Petrolina, PE, Brazil
[c] Department of Immunology, Laboratory of Immunopathology and Molecular Biology, IAM / FIOCRUZ, 50740-465, Recife, PE, Brazil
[d] Department of Biochemistry and Immunology, Institute of Biological Sciences, Federal University of Minas Gerais, 31270-901, Belo Horizonte, MG, Brazil
[e] Laboratory of Immunopathology Keizo Asami-LIKA / UFPE, 50670-420, Recife, PE, Brazil
[f] Department of Parasitology, Cellular and Molecular Biology Laboratories, Leishmaniasis, and Mutagenesis, IAM / FIOCRUZ, 50740-465, Recife, PE, Brazil

ARTICLE INFO

Keywords:
Chagas disease
Trypanosoma cruzi
Trypanocidal activity
Thiazolidinones

ABSTRACT

Chagas disease causes more deaths in the Americas than any other parasitic disease. Initially confined to the American continent, it is increasingly becoming a global health problem. In fact, it is considered to be an "exotic" disease in Europe, being virtually undiagnosed. Benznidazole, the only drug approved for treatment, effectively treats acute-stage Chagas disease, but its effectiveness for treating indeterminate and chronic stages remains uncertain. Previously, our research group demonstrated that 4-thiazolidinones presented anti-*T. cruzi* activity including in the *in vivo* assays in mice, making this fragment appealing for drug development. The present work reports the synthesis and anti-*T. cruzi* activities of a novel series of 4-thiazolidinones derivatives that resulted in an increased anti-*T. cruzi* activity in comparison to thiosemicarbazones intermediates. Compounds **2c, 2e,** and **3a** showed potent inhibition of the trypomastigote form of the parasite at low cytotoxicity concentrations in mouse splenocytes. Besides, all the **2c**, **2e**, and **3a** tested concentrations showed no cytotoxic activity on macrophages cell viability. When macrophages were submitted to *T. cruzi* infection and treated with **2c** and **3a,** compounds reduced the release of trypomastigote forms. Results also showed that the increased trypanocidal activity induced by **2c** and **3a** is independent of nitric oxide release. Flow cytometry assay showed that compound **2e** was able to induce necrosis and apoptosis in trypomastigotes. Parasites treated with the compounds **2e, 3a,** and **3c** presented flagellum shortening, retraction and curvature of the parasite body, and extravasation of the internal content. Together, these data revealed a novel series of 4-thiazolidinones fragment-based compounds with potential effects against *T. cruzi* and lead-like characteristics.

1. Introduction

Chagas disease, also known as American trypanosomiasis, is one of the main neglected diseases worldwide and a potentially life-threatening illness caused by the protozoan parasite *Trypanosoma cruzi* (*T. cruzi*) [1]. It is found mainly in 21 Latin American countries, where it is primarily vector-born. The primary vector involved in transmitting the parasite to humans is a triatomine bug, also known as a "kissing bug". 8 million people are estimated to be infected worldwide, mainly in Latin America [1,2]. Other means of transmission involve transfusion of contaminated blood and infected mothers to children during pregnancy or delivery (congenital transmission). Less frequently, organ transplantation or laboratory accidents can also result in transmission [3]. Population migration and tourism have distributed the disease into the United

* Corresponding author. laboratory of planning in medicinal chemistry - lpqm, Federal University Of Pernambuco, Health Sciences Center, Department Of Pharmaceutical Sciences, Arthur de Sá, S / N. University City. CEP, 50740-520, Recife, PE, Brazil.
E-mail address: ana.lleite@ufpe.br (A.C. Lima Leite).

https://doi.org/10.1016/j.cbi.2021.109514
Received 22 December 2020; Received in revised form 28 April 2021; Accepted 7 May 2021
Available online 21 May 2021

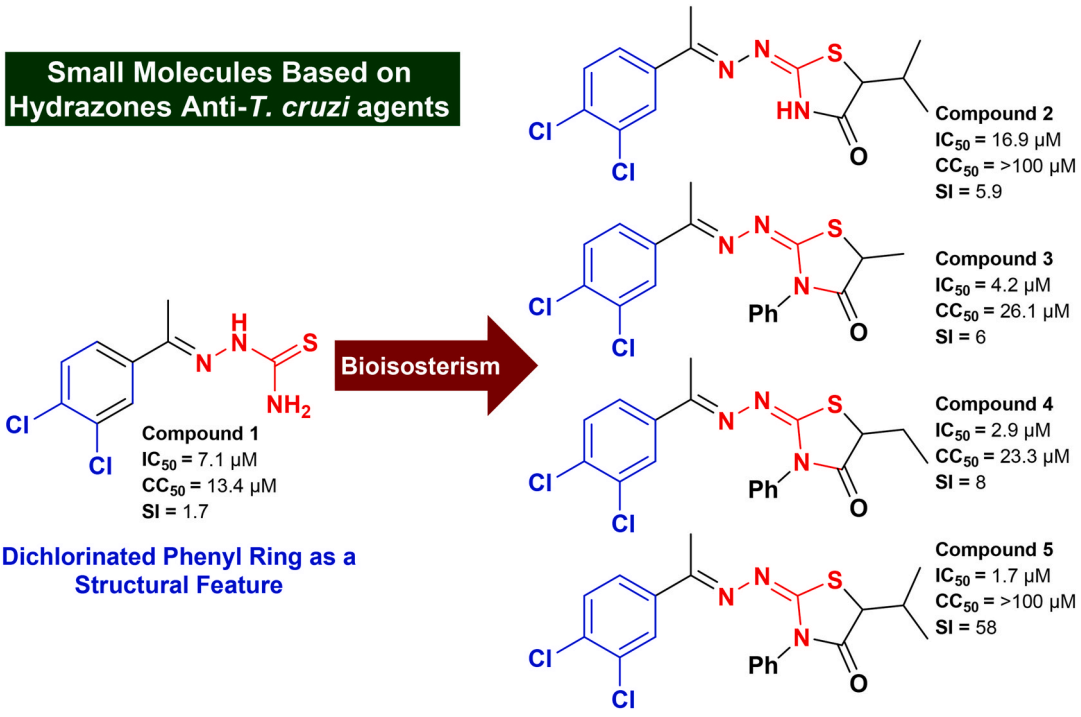

Fig. 1. Anti-*T. cruzi* agents based in 4-thiazolidinones (IC_{50} for trypomastigote form and CC_{50} for macrophages).

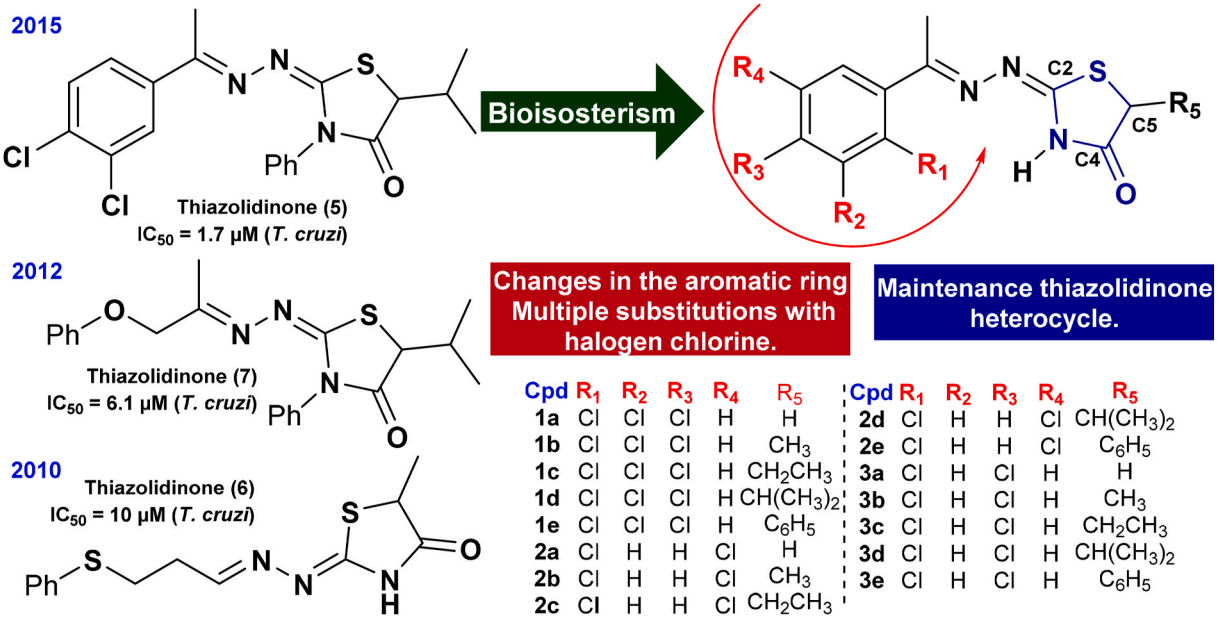

Cpd	R_1	R_2	R_3	R_4	R_5
1a	Cl	Cl	Cl	H	H
1b	Cl	Cl	Cl	H	CH_3
1c	Cl	Cl	Cl	H	CH_2CH_3
1d	Cl	Cl	Cl	H	$CH(CH_3)_2$
1e	Cl	Cl	Cl	H	C_6H_5
2a	Cl	H	H	Cl	H
2b	Cl	H	H	Cl	CH_3
2c	Cl	H	H	Cl	CH_2CH_3
2d	Cl	H	H	Cl	$CH(CH_3)_2$
2e	Cl	H	H	Cl	C_6H_5
3a	Cl	H	Cl	H	H
3b	Cl	H	Cl	H	CH_3
3c	Cl	H	Cl	H	CH_2CH_3
3d	Cl	H	Cl	H	$CH(CH_3)_2$
3e	Cl	H	Cl	H	C_6H_5

Fig. 2. Bioisosterism-based design of novel thiazolidinones as potential antiparasitic compounds. Thiazolidinones are described over the years, and thiazolidinones proposed here.

States, Europe, and Asia, which poses a growing risk to public health. Globalization and increased international travel and trade between endemic and non-endemic countries make Chagas disease a growing concern globally [1,3–5].

The only drugs accepted for clinical use are the two nitroheterocyclic compounds, Benznidazole (BDZ) and Nifurtimox (NFX), which are inadequate due to toxicity and low cure rates during the chronic stage of the disease. The lack of pharmaceutical company interest in developing anti-*T. cruzi* drugs make Chagas one of the major "neglected" diseases of the world [6,7]. The toxicity of these drugs is linked to their mode of action, and multiple undesired side effects inevitably accompany the treatment. From more than 1200 new drugs discovered between 1975 and 1997, only 4 resulted from a directed research and development effort by the pharmaceutical industry on treating human tropical disease, and 1 of those 4 (nifurtimox) is no longer in widespread use [7,8].

The urgent need for new therapeutic approaches is being met by a combined effort from the academic and commercial sectors, together with significant input from not-for-profit drug development consortia. With the disappointing outcomes of recent clinical trials against chronic Chagas disease, it has become clear that an incomplete understanding of parasite biology and disease pathogenesis impacts the development of more effective drugs. Also, technical issues, including difficulties in

establishing parasitological cures in human and animal models, have complicated drug efficacy assessments [9,10]. Therefore, it is of primordial importance the search for new compounds more active and selective against *T. cruzi*.

Over the years, our research group has investigated small molecules based on hydrazones (thiosemicarbazones, 4-thiazolidinones, and 1,3-thiazoles) to obtain novel and potent anti-*T. cruzi* agents [11–19]. In this way, 4-thiazolidinones derivatives have been largely investigated as anti-*T. cruzi* agents [13,18,19]. In recent work, we employed bioisosterism to modify a potent antiparasitic and cruzain-inhibitor dichlorinated phenyl-thiosemicarbazone (**1**) in a new series of 4-thiazolidinones (Fig. 1).

The antiparasitic activity on Y strain trypomastigotes form and host cell cytotoxicity in J774 macrophages revealed that compounds are more potent (**3–5**) and more selective (**2–5**) antiparasitic agents than thiosemicarbazone (**1**). In infected macrophages, compounds (**3**–**5**) reduced intracellular amastigotes, whereas Benznidazole did not. In *T. cruzi*-infected mice treated orally with 100 mg/kg of compound (**5**), a decrease of parasitemia was observed. These compounds present a dichlorinated phenyl ring as a structural feature, and the studies of the structure-activity relationship identified that the 3,4-dichlorophenyl moiety is a structural determinant for trypanocidal activity [13,20]. In fact, over the years, our research group has described generations of 4-thiazolidinones with promising anti-*T. cruzi* activity, including the *in vivo* assays in mice [13,19,21].

Based on this, in the present work, we have developed a new generation of 4-thiazolidinones, having as main structural characteristics: maintenance of thiazolidinone heterocycle, a di or tri-chlorophenyl-ethylidenehydrazone, and H or alkyl substituents in C5 position of thiazolidinone ring (Fig. 2). Compounds (**1a-e**, **2a-e**, and **3a-e**) were assayed for their *in vitro* anti-*T. cruzi* activity against trypomastigote and epimastigote forms. Their cytotoxicity in mammalian cell cultures was also investigated. The most active compounds were also evaluated against the intracellular form of the parasite, and the cell viability and confocal microscopy studies were also undertaken.

2. Materials and methods

2.1. Chemistry

All reagents were used as purchased from commercial sources (Sigma-Aldrich, Vetec, or Fluka). The progress of the reactions was followed by thin-layer chromatography (silica gel 60 F_{254} in aluminum foil). The purity of the target compounds was confirmed by combustion analysis (for C, H, N, and S) performed by a Carlo-Erba instrument (model EA 1110). IR was determined in KBr pellets. For NMR, we used Varian UnityPlus 400 MHz (400 MHz for ^{1}H and 100 MHz for ^{13}C) and Bruker AMX-300 MHz (300 MHz for ^{1}H and 75.5 MHz for ^{13}C) instruments. DMSO-d_6, acetone-d_6, and D_2O were purchased from CIL. Chemical shifts are reported in ppm, and multiplicities are given as s (singlet), d (doublet), t (triplet), q (quartet), m (multiplet), and dd (double doublet), with coupling constants (*J*) in Hertz. NH signals were localized in each spectrum after the addition of a few drops of D_2O. Structural assignments were corroborated by DEPT analysis, and Mass spectrometry experiments were performed on a Q-TOF spectrometer LC-IT-TOF (Shimadzu). When otherwise specified, ESI was carried out in the positive ion mode. Reactions in an ultrasound bath (QUIMIS) were carried out under a frequency of 40 kHz (180 W) and without external heating.

2.1.1. General procedure for the synthesis of thiosemicarbazones (1–3)

Example for compound (**1**): Synthesis of 1-(2,3,4-trichlorophenyl)-ethylidenethiosemicarbazone (**1**). Under ultrasound irradiation: in a 100 mL round-bottom flask, 8.95 mmol (0.815 g) of thiosemicarbazide, 8.95 mmol (2.0 g) of 2′,3′,4′-trichloroacetophenone, 7 drops of H_2SO_4, and 30 mL of ethanol were added and maintained in an ultrasound bath for 2 h. After cooling back to room temperature, the precipitate was permeated in a Büchner funnel with a sintered disc filter, washed with cold ethanol, and dried over SiO_2. The product was purified by recrystallization in hot toluol. Colorless crystals, m.p.: 230–232 °C; yield: 1.83 g (69%); IR (KBr): 3386 and 3286 (NH), 3172 (C–H, Ar), 3030 (C–H), 1602 (C═N) cm^{-1}. ^{1}H NMR (300 MHz, DMSO-d_6): δ 2.18 (s, 3H, CH_3), 7.29 (d, 1H, Ar), 7.41 (d, 1H, Ar), 7.72 (s, 1H, NH_2), 8.17 (s, 1H, NH), 10.44 (s, 1H, NH_2). ^{13}C NMR (75.5 MHz, DMSO-d_6): δ 18.26 (CH_3), 127.95 (CH, Ar), 129.50 (CH, Ar), 130.54 (C, Ar), 131.10 (C, Ar), 132.87 (C, Ar), 136.40 (C, Ar), 147.40 (C═N), 179.31 (C═S). Anal. calcd for $C_9H_8Cl_3N_3S$: C, 36.44; H, 2.72; N, 14.17; S, 10.81. Found: C, 36,16; H, 3,01; N, 14,09; S, 10,28.

1-(2,5-dichlorophenyl)ethylidenethiosemicarbazone (**2**). Recrystallization in hot toluol afforded colorless crystal, m.p.: 160 °C; yield: 1.77 g (64%); IR (KBr): 3441 and 3216 (NH), 3155 (C–H, Ar), 3020 (C–H), 1601 (C═N) cm^{-1}. ^{1}H NMR (300 MHz, DMSO-d_6): δ 2.19 (s, 3H, CH_3), 7.44 (d, 1H, Ar), 7.47 (d, 1H, Ar), 7.53 (s, 1H, Ar), 8.30 (s, 1H, NH), 9.50 (s, 1H, NH), 10.40 (s, 1H, NH_2). ^{13}C NMR (75.5 MHz, DMSO-d_6): δ 18.27 (CH_3), 129.84 (CH, Ar), 129.98 (CH, Ar), 130.35 (CH, Ar), 131.35 (C, Ar), 135.15 (C, Ar), 140.17 (C, Ar), 147.40 (C═N), 179.31 (C═S). HRMS (ESI): 262.0520 $[M+H]^+$. Anal. calcd for $C_9H_9Cl_2N_3S$: C, 41.23; H, 3.46; N, 16.03; S, 12.23. Found: C, 41.52; H, 2.95; N, 16.17; S, 12.28.

1-(2,4-dichlorophenyl)ethylidenethiosemicarbazone (**3**). Recrystallization in hot toluol afforded colorless crystal, m.p.: 210 °C; yield: 2.48 g (90%); IR (KBr): 3326 and 3286 (NH), 3172 (C–H, Ar), 3022 (C–H), 1601 (C═N) cm^{-1}. ^{1}H NMR (300 MHz, DMSO-d_6): δ 2.28 (s, 3H, CH_3), 7.63 (d, 1H, Ar), 7.89 (dd, 1H, Ar), 8.23 (d, 1H, H–Ar), 8.60 (s, 1H, NH), 8.62 (s, 1H, NH), 10.33 (s, 1H, NH_2). ^{13}C NMR (75.5 MHz, DMSO-d_6): δ 13.85 (CH_3), 126.75 (CH, Ar), 128.14 (CH, Ar), 130.24 (CH, Ar), 131.35 (C, Ar), 131.56 (C, Ar), 138.32 (C, Ar), 145.03 (C═N), 178.66 (C═S). Anal. calcd for $C_9H_9Cl_2N_3S$: C, 41.23; H, 3.46; N, 16.03; S, 12.23. Found: C, 41.68; H, 2.58; N, 16.21; S, 11.69.

2.1.2. General procedure for the synthesis of thiazolidinones (1a-3e)

Example for compound (**1a**). Synthesis of 2-[1-(2,3,4-trichlorophenyl)ethylidenohydrazone]thiazolidin-4-one (**1a**). In a 100 mL round-bottom flask, 1.7 mmol (0.5 g) of thiosemicarbazone (**1**) was dissolved in 30 mL of ethanol, followed by adding 6.8 mmol (0.557 g) anhydrous sodium acetate under magnetic stirring and warming. After 15 min, 3.4 mmol (0.567 g) of ethyl 2-bromoacetate was added in portions, and the mixture was maintained under reflux for 24 h. After cooling back to rt, the precipitate was filtered in a Büchner funnel with a sintered disc filter, washed with cold ethanol and water, and dried over SiO_2. The product was purified by recrystallization in hot cyclohexane. Colorless crystals were obtained. M.p: 210 °C; yield: 0.31 g (54%); IR (KBr): 3117 (NH), 2968 (C–H), 1715 (C═O), 1637 (C═N) cm^{-1}. ^{1}H NMR (300 MHz, DMSO-d_6): δ 2.29 (s, 3H, CH_3), 3.83 (s, 2H, S–CH_2, heterocycle), 7.41 (d, 1H, Ar), 7.62 (d, 1H, Ar), 11.99 (s, 1H, NH). ^{13}C NMR and DEPT (75.5 MHz, DMSO-d_6): 18.67 (CH_3), 32.7 (CH_2, heterocycle), 127.95 e (CH, Ar), 128.94 e (CH, Ar), 129.50 (C, Ar), 131.11 (C, Ar), 133.00 (C, Ar), 135.40 (C, Ar), 160.64 (C═N), 166.31 (S–C═N), 174.18 (C═O). Anal. calcd for $C_{11}H_8Cl_3N_3OS$: C, 39.25; H, 2.40; N, 12.48; S, 9.52. Found: C, 39.06; H, 2.47; N, 12.54; S, 9.11.

2-[1-(2,3,4-trichlorophenyl)ethylidenohydrazone]-5-methyl-thiazolidin-4-one (**1b**). Recrystallization in toluol \ cyclohexane 2:1 afforded colorless crystals. M.p: 210 °C; yield: 0.29 g (49%); IR (KBr): 3153 (NH), 2963 (C–H), 1744 (C═O), 1623 (C═N) cm^{-1}. ^{1}H NMR (300 MHz, DMSO-d_6): δ 1.55 (d, 3H, CH_3 heterocycle), 2.33 (s, 3H, CH_3), 4.10 (q, 1H, CH heterocycle), 4.51 (s, NH), 7.40 (d, 1H,Ar), 7.61 (d, 1H,Ar). ^{13}C NMR (75.5 MHz, DMSO-d_6): δ 19.36 (CH_3 heterocycle), 23.01 (CH_3), 43.21 (CH, heterocycle), 129.60 (CH, Ar), 130.98(CH, Ar), 132.65 (C, Ar), 134.37 (C, Ar), 135.15 (C, Ar), 140.17 (C, Ar), 161.71 (C═N), 179.31 (S–C═N), 175.01 (C═O). HRMS (ESI): 350.0332 $[M+H]^+$. Anal. calcd for $C_{12}H_{10}Cl_3N_3OS$: C, 41.11; H, 2.87; N, 11.78; S, 9.14. Found: C, 41.46; H, 3.13; N, 12.16; S, 9.58.

2-[1-(2,3,4-trichlorophenyl)ethylidenohydrazone]-5-

ethylthiazolidin-4-one (**1c**). Recrystallization in hot toluol afforded colourless crystals. M.p: 183 °C; yield: 0.35 g (57%); IR (KBr): 3149 (NH), 2974 (C–H), 1717 (C═O), 1627 (C═N) cm^{-1}. ^1H NMR (300 MHz, DMSO-d_6): δ 2.20 (t, 3H, CH_3), 2.20 (m, 1H, CH_2), 2.52 (s, 3H, CH_3), 3.83 (dd, 1H, CH heterocycle), 7.58 (d, 1H, Ar), 7.81 (d, 1H, Ar), 10.40 (s, 1H, NH). ^{13}C NMR (75.5 MHz, DMSO-d_6): δ 10.88 (CH_3), 18.87 (CH_3), 26.88 (CH_2), 50.20 (CH, heterocycle), 129.63 (CH, Ar), 130.02 (CH, Ar), 132.67 (C, Ar), 133.77 (C, Ar), 134.43 (C, Ar), 141.10 (C, Ar), 162.31 (C═N), 164.40 (S–C═S), 176.12 (C═O). HRMS (ESI): 364.0919 $[M+H]^+$. Anal. calcd for $C_{13}H_{12}Cl_3N_3OS$: C, 42.82; H, 3.32; N, 11.52; S, 8.79. Found: C, 42.56; H, 3.23; N, 11.36; S, 8.83.

2-[1-(2,3,4-trichlorophenyl)ethylidenohydrazone]-5-isopropylthiazolidin-4-one (**1d**). Recrystallization in hot toluol afforded colorless crystals. M.p: 232 °C; yield: 0.51 g (80%); IR (KBr): 3141 (NH), 2964 (C–H), 1716 (C═O), 1631 (C═N) cm^{-1}. ^1H NMR (300 MHz, DMSO-d_6): δ 0.85 (d, 3H, CH_3), 0.95 (d, 3H, CH_3), 2.35 (s, 3H, CH_3), 3.31 (m, 1H, CH), 4.27 (d, 1H, CH heterocycle), 7.43 (d, 1H, Ar), 7.69 (d, 1H, Ar), 12.02 (s,1H, NH). ^{13}C NMR (75.5 MHz, DMSO-d_6): δ 16.36 (CH_3), 18.69 (CH_3), 20.29 (CH_3), 29.78 (CH), 54.65 (CH, heterocycle), 127.31 (CH, Ar), 129.03 (CH, Ar), 130.73 (C, Ar), 131.12 (C, Ar), 133.04 (C, Ar), 135.15 (C, Ar), 161.12 (C═N), 164.06 (S–C═N), 175.35 (C═O). HRMS (ESI): 378.0726 $[M+H]^+$. Anal. calcd for $C_{14}H_{14}Cl_3N_3OS$: C, 44.40; H, 3.73; N, 11.10; S, 8.47. Found: C, 44.25; H, 3.63; N, 10.77; S, 8.04.

2-[1-(2,3,4-trichlorophenyl)ethylidenohydrazone]-5-phenylthiazolidin-4-one (**1e**). Recrystallization in hot toluol afforded colorless crystals. M.p: 202 °C; yield: 0.45 g (64%); IR (KBr): 3428 (NH), 1711 (C═O), 1625 (C═N) cm^{-1}. ^1H NMR (300 MHz, DMSO-d_6): δ 2.32 (s, 3H, CH_3), 3.45 (s, NH), 5.31 (s, 1H, CH heterocycle), 7.33 (m, 5H, Ar), 7.41 (d, 1H,Ar), 7.70 (d, 1H,Ar). 2.41 (s, 3H, CH_3), 5.49 (s, 1H, CH heterocycle), 7.39 (m, 5H, Ar), 7.68 (d, 1H, *J* 9 Hz, Ar), 7.81 (dd, 1H, *J* 9 and 2.25 Hz, Ar), 8.01 (d, 1H, *J* 2.25 Hz, Ar), 12.35 (s, 1H, NH). ^{13}C NMR (75.5 MHz, DMSO-d_6): δ 21.07 (CH3), 52.16 (CH, heterocycle), 127.71 (CH, Ar), 128.62 (CH, Ar), 129.12 (CH, Ar), 130.34 (C, Ar), 131.17 (CH, Ar), 132.19 (CH, Ar), 132.77 (CH, Ar), 137.41 (C, Ar), 137.98 (C, Ar), 139.97(C, Ar), 158.12 (C═N), 171.99 (S–C═N), 177.87 (C═O). HRMS (ESI): 412.0927 $[M+H]^+$. Anal. calcd for $C_{17}H_{12}Cl_3N_3OS$: C, 49.47; H, 2.93; N, 10.18; S, 7.77. Found: C, 49.68; H, 3.16; N, 10.01; S, 7.54.

2-[1-(2,5-dichlorophenyl)ethylidenohydrazone]thiazolidin-4-one (**2a**). Recrystallization in hot toluol/cyclohexane 1:1 afforded colorless. M.p: 180 °C; yield: 0.4 g (70%); IR (KBr): 3415 (NH), 2915 (C–H), 1715 (C═O), 1631 (C═N) cm^{-1}. ^1H NMR (300 MHz, DMSO-d_6): δ 2.30 (s, 3H, CH_3), 3.85 (s, 2H, S–CH_2, heterocycle), 7.49 (d, 1H, Ar), 7.52 (d, 1H, Ar), 7.57 (s, 1H, Ar) 11.98 (s,1H, NH). ^{13}C NMR and DEPT (75.5 MHz, DMSO-d_6): 18.74 (CH_3), 33.35 (CH_2, heterocycle), 128.61 (CH, Ar), 129.85 (CH, Ar), 129.98 (CH, Ar), 131.37 (C, Ar), 131.81 (C, Ar), 147.42 (C, Ar), 152.40 (C═N), 172.31 (S–C═N), 179.7 (C═O). HRMS (ESI): 302.0331 $[M+H]^+$. Anal. calcd for $C_{11}H_9Cl_2N_3OS$: C, 43.72; H, 3.00; N, 13.91; S, 10.61. Found: C, 43.53; H, 3.28; N, 13.64; S, 10.58.

2-[1-(2,5-dichlorophenyl)ethylidenohydrazone]-5-methylthiazolidin-4-one (**2b**). Recrystallization in hot cyclohexane afforded colorless crystals. M.p: 182 °C; yield: 0.36 g (60%); IR (KBr): 3141 (NH), 2968 (C–H), 1716 (C═O), 1630 (C═N) cm^{-1}. ^1H NMR (300 MHz, DMSO-d_6): δ 1.39 (d, 3H, CH_3 heterocycle), 1.88 (s, 3H, CH_3), 3.81 (q, CH heterocycle), 7.44 (d, 1H, Ar), 7.51 (d, 1H, Ar), 7.60 (s, 1H, Ar), 9.50 (s, 1H, NH). ^{13}C NMR (75.5 MHz, DMSO-d_6): δ 18.42 (CH_3 heterocycle), 21.40 (CH_3), 43.70 (CH heterocycle), 129.34 (CH, Ar), 129.80(CH, Ar), 129.88 (CH, Ar), 131.49 (C, Ar),131.56 (C, Ar), 141.04(C, Ar), 155.78 (C═N), 172.16 (S–C═N), 183.54 (C═O). Anal. calcd for $C_{12}H_{11}Cl_2N_3OS$: C, 45.58; H, 3.51; N, 13.29; S, 10.14. Found: C, 45.12; H, 3.57; N, 13.49; S, 10.35.

2-[1-(2,5-dichlorophenyl)ethylidenohydrazone]-5-ethylthiazolidin-4-one (**2c**). Recrystallization in hot toluol/cyclohexane 2:1 afforded colorless crystals. M.p: 175 °C; yield: 0.55 g (87%); IR (KBr): 3126 (NH), 2961 (C–H), 1709 (C═O), 1601 (C═N) cm^{-1}. ^1H NMR (300 MHz, DMSO-d_6): δ 0.89 (t, 3H, CH_3), 1.63 (m, 1H, CH_2), 1.91 (m, 1H, CH_2), 2.26 (s, 3H, CH_3), 3.53 (dd, 1H, CH heterocycle), 7.22 (d, 1H, Ar), 7.46 (d, 1H, Ar), 7.53 (s, 1H, Ar), 8.30 (s, 1H, NH). ^{13}C NMR (75.5 MHz, DMSO-d_6): δ 11.27 (CH_3), 16.98 (CH_3), 27.45 (CH_2), 51.14 (CH, heterocycle), 128.16 (CH, Ar), 129.33 (CH, Ar), 129.89 (CH, Ar), 131.46 (C, Ar), 131.45 (C, Ar), 141.17 (C, Ar), 155.87 (C═N), 172.22 (S–C═N), 182.4 (C═O). Anal. calcd for $C_{13}H_{13}Cl_2N_3OS$: C, 47.28; H, 3.97; N, 12.72; S, 9.71. Found: C, 47.11; H, 3.77; N, 12.88; S, 9.51.

2-[1-(2,5-dichlorophenyl)ethylidenohydrazone]-5-isopropylthiazolidin-4-one (**2d**). Recrystallization in hot toluol/cyclohexane 2:1 afforded colorless crystals. M.p: 190 °C; yield: 0.30 g (45%); IR (KBr): 3418 (NH), 1703 (C═O), 1645 (C═N) cm^{-1}. ^1H NMR (300 MHz, DMSO-d_6): δ 0.87 (d, 3H, CH_3), 0.95 (d, 3H, CH_3), 2.27 (s, 3H, CH_3), 3.41 (m, 1H, CH), 4.57 (d, 1H, CH heterocycle), 7.40 (d, 1H, Ar), 7.71 (d, 1H, Ar), 7.88 (s, 1H, Ar), 12.09 (s,1H, NH). ^{13}C NMR (75.5 MHz, DMSO-d_6): δ 15.33 (CH_3), 17.69 (CH_3), 21.27 (CH_3), 27.78 (CH), 53.66 (CH, heterocycle), 128.31 (CH, Ar), 129.03 (CH, Ar), 130.99 (C, Ar), 132.12 (C, Ar), 133.04 (C, Ar), 135.15 (C, Ar), 162.12 (C═N), 165.06 (S–C═N), 175.35 (C═O). Anal. calcd for $C_{14}H_{15}Cl_2N_3OS$: C, 48.85; H, 4.39; N, 12.21; S, 9.31. Found: C, 48.44; H, 4.18; N, 12.57; S, 9.38.

2-[1-(2,5-dichlorophenyl)ethylidenohydrazone]-5-phenylthiazolidin-4-one (**2e**). Recrystallization in hot toluol afforded colorless crystals. M.p: 160 °C; yield: 0.36 g (50%); IR (KBr): 3275 (NH), 2998 (C–H), 1750 (C═O), 1602 (C═N) cm^{-1}. ^1H NMR (300 MHz, DMSO-d_6): δ 2.27 (s, 3H, CH_3), 4.07 (s, NH), 4.75 (s, 1H, CH heterocycle), 7.33 (m, 5H, Ar), 7.40 (d, 1H, Ar), 7.71 (d, 1H, Ar), 7.88 (s, 1H, Ar). ^{13}C NMR (75.5 MHz, DMSO-d_6): δ 18.33 (CH_3), 54.85 (CH, heterocycle), 126.71 (CH, Ar), 128.62 (CH, Ar), 128.88 (CH, Ar), 128.99 (C, Ar), 129.92 (CH, Ar), 129.97 (CH, Ar), 131.45 (CH, Ar), 141.41 (C, Ar), 141.98 (C, Ar), 142.97(C, Ar), 152.68 (C═N), 172.35 (S–C═N), 179.88 (C═O). HRMS (ESI): 376.3217 $[M+H]^+$. Anal. calcd for $C_{17}H_{13}Cl_2N_3OS$: C, 53.98; H, 3.46; N, 11.11; S, 8.48. Found: C, 53.88; H, 3.10; N, 11.34; S, 8.20.

2-[1-(2,4-dichlorophenyl)ethylidenohydrazone]thiazolidin-4-one (**3a**). Recrystallization in hot cyclohexane afforded colorless. M.p: 203 °C; yield: 0.35 g (62%); IR (KBr): 3171 (NH), 2950 (C–H), 1721 (C═O), 1633 (C═N) cm^{-1}. ^1H NMR (300 MHz, DMSO-d_6): δ 2.43 (s, 3H, CH_3), 3.95 (s, 2H, S–CH_2, heterocycle), 7.72 (d, 1H, Ar), 7.83 (dd, 1H, Ar), 8.03 (d, 1H, Ar). ^{13}C NMR and DEPT (75.5 MHz, DMSO-d_6): 14.24 (CH_3), 32.01 (CH_2, heterocycle) 126.35 (CH, Ar), 127.91 (CH, Ar), 130.54 (CH, Ar), 131.26 (C, Ar), 132.31 (C, Ar), 138.18 (C, Ar), 159.42 (C═N), 164.53 (S–C═N), 172.04 (C═O). Anal. calcd for $C_{11}H_9Cl_2N_3OS$: C, 43.72; H, 3.00; N, 13.91; S, 10.61. Found: C, 43.33; H, 3.78; N, 13.44; S, 10.78.

2-[1-(2,4-dichlorophenyl)ethylidenohydrazone]-5-methylthiazolidin-4-one (**3b**). Recrystallization in hot toluol/cyclohexane 2:1 afforded colorless crystals. M.p: 170 °C; yield: 0.31 g (51%); IR (KBr): 3141 (NH), 1741 (C═O), 1627 (C═N) cm^{-1}. ^1H NMR (300 MHz, DMSO-d_6): δ 1.38 (d, 3H, CH_3), 2.25 (s, 3H, CH_3), 3.81 (q, 1H, CH heterocycle), 4.20 (s, 1H, NH), 7.40 (d, 1H, Ar), 7.48 (d, 1H, Ar), 7.64 (s, 1H, Ar). ^{13}C NMR (75.5 MHz, DMSO-d_6): δ 18.54 (CH_3), 21.47 (CH_3), 43.59 (CH heterocycle), 127.30 (CH, Ar), 129.16(CH, Ar), 131.67 (CH, Ar), 132.12 (C, Ar),133.36 (C, Ar), 138.32(C, Ar), 156.26 (C═N), 172.21 (S–C═N), 183.08 (C═O). Anal. calcd for $C_{12}H_{11}Cl_2N_3OS$: C, 45.58; H, 3.51; N, 13.29; S, 10.14. Found: C, 45.32; H, 3.17; N, 13.02; S, 10.47.

2-[1-(2,5-dichlorophenyl)ethylidenohydrazone]-5-ethylthiazolidin-4-one (**3c**). Recrystallization in hot toluol afforded colorless crystals. M.p: 120 °C; yield: 0.30 g (47%); IR (KBr): 3155 (NH), 2964 (C–H), 1726 (C═O), 1625 (C═N) cm^{-1}. ^1H NMR (300 MHz, DMSO-d_6): δ 0.92 (t, 3H, CH_3), 1.80 (m, 1H, CH_2), 1.94 (m, 1H, CH_2), 2.23 (s, 3H, CH_3), 4.16 (dd, 1H, CH heterocycle), 7.30 (d, 1H, Ar), 7.46 (d, 1H, Ar), 7.68 (s, 1H, Ar), 11.94 (s, 1H, NH). ^{13}C NMR (75.5 MHz, DMSO-d_6): δ 10.35 (CH_3), 18.73 (CH_3), 25.45 (CH_2), 48.75 (CH, heterocycle) 127.84 (CH, Ar), 128.98 (CH, Ar), 130.05 (CH, Ar), 131.75 (C, Ar), 135.15 (C, Ar), 140.17 (C, Ar), 159.06 (C═N), 163.81 (S–C═N), 175.92 (C═O). Anal. calcd for $C_{13}H_{13}Cl_2N_3OS$: C, 47.28; H, 3.97; N, 12.72; S, 9.71. Found: C, 47.02; H, 3.98; N, 12.62; S, 9.32.

2-[1-(2,4-dichlorophenyl)ethylidenohydrazone]-5-isopropylthiazolidin-4-one (**3d**). Recrystallization in hot toluol/cyclohexane 2:1 afforded colorless crystals. M.p: 190 °C; yield: 0.25 g (38%); IR (KBr): 3420 (NH), 1752 (C═O), 1640 (C═N) cm^{-1}. ^{1}H NMR (300 MHz, DMSO-d_6): δ 0.88 (d, 3H, CH_3), 0.97 (d, 3H, CH_3), 2.33 (s, 3H, CH_3), 3.51 (m, 1H, CH), 5.07 (d, 1H, CH heterocycle), 7.50 (d, 1H, Ar), 7.81 (d, 1H, Ar), 7.98 (s, 1H, Ar), 8.2 (s,1H, NH). ^{13}C NMR (75.5 MHz, DMSO-d_6): δ 16.33 (CH_3), 18.29 (CH_3), 22.87 (CH_3), 27.78 (CH), 86.08 (CH, heterocycle), 127.31 (CH, Ar), 129.03 (CH, Ar), 130.08 (C, Ar), 132.13 (C, Ar), 133.04 (C, Ar), 135.15 (C, Ar), 160.12 (C═N), 164.06 (S–C═N), 176.35 (C═O). HRMS (ESI): 376.0030 $[M - H]^+$. Anal. calcd for $C_{14}H_{15}Cl_2N_3OS$: C, 48.85; H, 4.39; N, 12.21; S, 9.31. Found: C, 48.22; H, 4.08; N, 12.77; S, 9.38.

2-[1-(2,4-dichlorophenyl)ethylidenohydrazone]-5-phenylthiazolidin-4-one (**3e**). Recrystallization in hot toluol afforded colourless crystals. MP: 170 °C; yield: 0.32 g (45%); IR (KBr): 3141 (NH), 1920 (C–H), 1721 (C═O), 1628 (C═N) cm^{-1}. ^{1}H NMR (300 MHz, DMSO-d_6): 2.32 (s, 3H, CH_3), 5.24 (s, 1H, CH heterocycle) 7.55 (m, 5H, Ar), 7.67 (d, 1H, Ar), 7.89 (d, 1H, Ar), 8.2 (s, 1H, Ar), 9.5 (s,1H, NH). ^{13}C NMR (75.5 MHz, DMSO-d_6): δ 19.74 (CH_3), 54.50 ($CH_,$ heterocycle), 126.71 (CH, Ar), 127.62 (CH, Ar), 129.12 (CH, Ar), 131.34 (C, Ar), 131.57 (CH, Ar), 132.19 (CH, Ar), 132.87 (CH, Ar), 137.41 (C, Ar), 137.98 (C, Ar), 139.97 (C, Ar), 152.40 (C═N), 168.31 (S–C═N), 172.07 (C═O). Anal. calcd for $C_{17}H_{13}Cl_2N_3OS$: C, 53.98; H, 3.46; N, 11.11; S, 8.48. Found: C, 53.70; H, 3.00; N, 11.01; S, 8.78.

2.2. Biology

2.2.1. Parasites

Epimastigotes of a Dm28c strain were maintained at 27 °C in liver infusion tryptose (LIT) medium supplemented with 10% fetal bovine serum (FBS, Cultilab). *T. cruzi* trypomastigotes (Y strain) were cultured on *Macaca mulatta* fibroblast cells line (LLCMK2) in culture flasks (TPP) with *Roswell Park Memorial Institute* 1640 medium (RPMI) supplemented with 5% of FBS, 1% L-glutamine (200 mM), and 1% penicillin and 1% streptomycin.

2.2.2. Activity against epimastigotes and trypomastigotes

Epimastigotes were counted in a hemocytometer and dispensed into 96-well plates at 10^5 cells/well. Trypomastigotes were counted and adjusted to 4×10^5 cells/well into a 96-well plate. Compounds were added in ten dilutions (0.19–100 μg/mL) in triplicate. Epimastigotes plates were incubated for 96 h at 27 °C, trypomastigotes plates, for 24 h, at 37 °C. In both assays, wells without compounds and treated with Benznidazole were used as negative and positive controls, respectively. After incubation, parasites were quantified using a Neubauer chamber. The percentage of inhibition was calculated using untreated cultures, and IC_{50} was calculated using non-linear regression on Prism 5.0 (GraphPad).

2.2.3. Cytotoxicity in mice spleen cells

Splenocytes were collected from BALB/c mice and cultivated in RPMI- 1640 medium supplemented with 10% FBS. The cells were placed into 96-well plates at 5×10^6 cells/well. Compounds were added in six dilutions (1, 5, 10, 25, 50, and 100 μg/mL), and wells without compounds and with saponin were used as negative and positive controls, respectively. [^{3}H]-thymidine (1.0 μCi/mL, PerkinElmer, Waltham, MA, USA) was added to each well, and plates were incubated for 24 h at 37 °C and 5% CO_2. Cells were then transferred to a filter paper using a cell harvester and quantified using a liquid scintillation counter (WALLAC 1209, Rackbeta Pharmacia, Stockholm, Sweden). [3H]-Thymidine incorporation [%] was measured, and the cytotoxic concentration (DL50) was determined using non-linear regression on Prism 5.0 (GraphPad).The assay was conducted in triplicate.

2.2.4. Macrophage culture, T. cruzi infection, MTT and nitric oxide (NO) evaluation

Macrophages (MO) were harvested from the peritoneal cavity of eight to ten weeks old female C57BL/6 mice three days after injection of 2 ml of 3% sodium thioglycolate. The cells were collected by washing the peritoneal cavity using sterile phosphate-buffered saline (PBS), centrifuged at 290 xg for 10 minutes, resuspended in a volume of 1mL of medium (RPMIc). The cells were counted in Neubauer's chamber and cultured ($2x10^6$ cells/well) in RPMIc. The adherent cells were obtained after 3 hours of incubation of single-cell suspensions in tissue culture plates (24 wells) at 37 o C in 5%. Nonadherent cells were removed and trypomastigotes forms were added at a 5:1 parasite-to-cells ratio to macrophages for 2 hours after the extracellular parasites were removed, and the cells were incubated at 37 o C in 5% CO_2 in the presence or absence of **2c**, **2e**, and **3a** (3.125, 6.25, 12.5, 25 and 50 μM) or with recombinant murine IFN-γ (100 ng/mL - Sigma). They were maintained throughout the remainder of the oven experiment at 37°C, 5% CO_2 . The supernatants were harvested 72 hours or 7 days post-infection (p.i.) and/or stimuli and assayed for nitrite concentration (72 h p.i.) by mixing 0.1 mL of culture supernatant with 0.1 mL of Griess reagent. Absorbance at 540 nm was read 10 minutes later, and NO_2 - concentration was determined. The MTT was evaluated by adding methanesulfonyl and methane dimethyl (oxide) sulfur at a 2mg/mL MTT solution to supernatants (7 days p.i.) for 90 min at 37°C. After this period, the MTT was withdrawn from the wells, and 1.500μL of dimethyl sulfoxide (DMSO) (Synth) was added. Triplicates of all samples (200μL/well) were placed in a 96-well plate, and the absorbance at 490nm was read, with MTT concentration determined. Macrophages were infected, the extracellular parasites were removed, and the cells were incubated with or without **2c**, **2e**, and **3a**. Parasite growth was evaluated by daily counting the trypomastigotes in the supernatant of infected macrophages on days 3 to 7 post-infection.

2.2.5. Cell death assessment

After confirmation of trypanocidal activity, Annexin-FITC/Propidium Iodide labeling was used to characterize cell death modalities induced by incubation with compounds. Metacyclic trypomastigotes were collected and seeded at 4x105 cells/well in RPMI-1640 medium. All compounds were dissolved in DMSO and added to wells at IC50 and 2x IC50 concentrations. Benznidazole (IC50 and 2x IC50) and culture medium were used as positive and negative control, respectively. Plates were incubated at the same conditions used for anti-trypomastigote activity (37 °C, 24 hours). Briefly, after treatment, parasites were washed with PBS and resuspended in binding buffer (Annexin V Binding Buffer- BD Pharmingen™, USA). For labeling, 10 mL of propidium iodide (50 mg/mL) and 5 mL of Annexin-FITC (BD Pharmingen™, USA) were added for 15 min, at room temperature, in dark. Flow cytometry was conducted in FACSCalibur (Becton & Dickinson, USA). For each sample we acquire 20,000 events and the data were analyzed using Cell Quest software (Becton & Dickinson, USA). Assays were conducted in triplicate. For significance analysis was used ANOVA and Dunnett's test, considering $p < 0.05$.

2.2.6. Ultrastructural analysis

The parasites were cultured for 24 h in RPMI 1640 medium (Sigma-Aldrich, St. Louis, MO, USA) buffered to pH 7.5 and supplemented with HEPES (20 mM), 10% fetal bovine serum, penicillin (100 U/mL), and streptomycin (100 mg/mL) containing the compound at the IC_{50} concentration and twice the value of IC_{50}. The parasites were collected, washed in PBS, and fixed with 2.5% glutaraldehyde, 4% formaldehyde, and 0.1 M cacodylate buffer at pH 6.8. They were then postfixed in 2% osmium tetroxide (OsO_4) in a 0.1 M cacodylate buffer at pH 6.8 and processed for routine scanning electron microscopy (SEM). The parasites were dehydrated in graded ethanol and dried by the critical point method with CO_2. The samples were mounted on aluminum stubs, coated with gold, and examined under a JEOL-5600LV microscope.

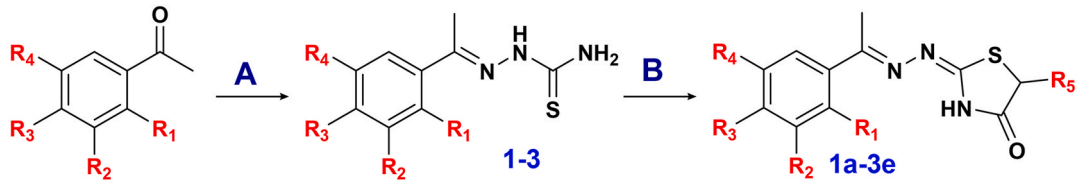

Compd.	R_1	R_2	R_3	R_4	R_5
1	Cl	Cl	Cl	H	-
2	Cl	H	H	Cl	-
3	Cl	H	Cl	H	-
1a	Cl	Cl	Cl	H	H
1b	Cl	Cl	Cl	H	CH_3
1c	Cl	Cl	Cl	H	CH_2CH_3
1d	Cl	Cl	Cl	H	$CH(CH_3)_2$
1e	Cl	Cl	Cl	H	C_6H_5
2a	Cl	H	H	Cl	H
2b	Cl	H	H	Cl	CH_3
2c	Cl	H	H	Cl	CH_2CH_3
2d	Cl	H	H	Cl	$CH(CH_3)_2$
2e	Cl	H	H	Cl	C_6H_5
3a	Cl	H	Cl	H	H
3b	Cl	H	Cl	H	CH_3
3c	Cl	H	Cl	H	CH_2CH_3
3d	Cl	H	Cl	H	$CH(CH_3)_2$
3e	Cl	H	Cl	H	C_6H_5

Scheme 1. Synthetic procedures for thiazolidinones (**1a-3e**). Reagents and conditions: (**A**) thiosemicarbazide, EtOH, H_2SO_4, ultrasound bath, rt, 1–2 h, yields of 64–90%; (**B**) ethyl 2-bromoacetate or ethyl 2-substituted-2-bromoacetates; NaOAc, EtOH, reflux, overnight, yields of 38–87%.

3. Results and discussion

3.1. Synthesis and chemical characterization

The general route to preparing 4-thiazolidinones is shown in Scheme 1. First, thiosemicarbazones (**1–3**) were prepared by reacting commercially available di- and trichloroacetophenones with the thiosemicarbazide in an ultrasound bath in the presence of catalytic H_2SO_4. The 4-thiazolidinones (**1a-3e**) were prepared by reacting to the respective aryl thiosemicarbazone (**1–3**) with commercially available ethyl 2-bromoacetate or by preparing [22] the desired 2-substituted-2--bromoacetates. These reactions were carried out in the presence of an excess of anhydrous NaOAc under reflux. This afforded compounds (**1a-3e**) in variable yields (38–87%) and acceptable purity (>95%).

Structures of compounds were determined by nuclear magnetic resonance (NMR-^{1}H, and ^{13}C), infrared (IR), and mass (HR-MS) spectra, while purity was determined by elemental analysis (EA).

An important structural feature of the compounds (**1a-3e**) is the position of thedouble bond involving the C2 carbon of the heterocyclic ring. Depending on the imino lactam tautomerism, the double bond of the C2 carbon present in the compounds may be endocyclic or exocyclic to the heterocycle (Fig. 3).

For an unambiguous assignment of this connection, we tried to obtain crystals of the compounds (**1a-3e**) suitable for the diffraction of X-rays, but we did not succeed. Taking account of our previous work (2015) [13] identified by X-ray crystallography that the position of the iminic bond in thiazolidinone heterocycle ring is located in an exocyclic position and adopts an *E*-geometry; therefore, we suggest that for these new compounds (**1a-3e**) this should be the accepted (Fig. 3) as observed for the 4-thiazolidinones previous crystallized [13].

3.2. Cytotoxicity

First, thiosemicarbazones 1-3 and 4-thiazolidinones 1a-3e toxicity to splenic cells of BALB/c mice were evaluated. As observed in Table 1, the cytotoxicity of the thiosemicarbazone 3 (2,4-dichloro) for splenic cells was low (DL50= 3.83μM) and could be compared to that of nifurtimox (DL50= 3.48μM). In general, we observed that cyclization is beneficial since cyclic compounds presented less cytotoxic than their non-cyclic bioisosteres. This data corroborates with our previous studies, once the cyclization generates less toxic and more selective compounds [13, 23]. The only exceptions are thiazolidinones **1e** (DL_{50} = 24.33 μM) and **2e** (DL_{50} = 13.26 μM), which presents a phenyl ring at C5 position heterocyclic ring, suggesting that the lipophilic profile could influence this cytotoxic property of these compounds.

3.3. Antiparasitic activity against extracellular form

After assessing the host cell cytotoxicity in mouse splenocytes, the *in vitro* anti-*T. cruzi* activity was determined against trypomastigotes of Y strain and epimastigotes of DM28c strain (Table 1). Compounds that showed IC_{50} values comparable to Benznidazole were considered active.

The observed trypanocidal activity in unsubstituted thiosemicarbazones (**1–3**) was kept in their cyclic derivatives. They also presented lower cytotoxicity for splenocytes in opposition to thiosemicarbazones (**2** and **3**). Among cyclic derivatives, compounds (**1a**, **2c**, **2e**, and **3a-c**) present the same or better trypanocidal activity than thiosemicarbazones (**2–3**). We can analyze the structure-activity relations by dividing the sub-series of compounds (**1a-e**, **2a-e,** and **3a-e**).

For the sub-series (**1a-e**), we noted that substitutions at the C5 position of the heterocyclic ring were not beneficial for trypanocidal activity. This data may be related to the presence of the tri-chlorinated aromatic ring of this sub-series, which may be causing some steric hindrance in the target site, causing substitutions that increase the size of the analog to render it inactive. We can highlight the **1a** analog of this sub-series, which presents the unsubstituted thiazolidinone ring at C5 position and an IC_{50} = 9.20 μM, equipotent to Benznidazole.

For sub-series (**2a-e**), we observed that the analogs **2c** (IC_{50} = 4.99 μM) and **2e** (IC_{50} = 0.84 μM) were the most active of this sub-series; they present an ethyl and phenyl group respectively at the C5 position of the thiazolidinone ring. We can suppose that these groups have improved trypanocidal activity by increasing hydrophobic interactions in the target site of the parasite. This data corroborates with our previous studies, where the insertion of hydrophobic groups in the C5 position of

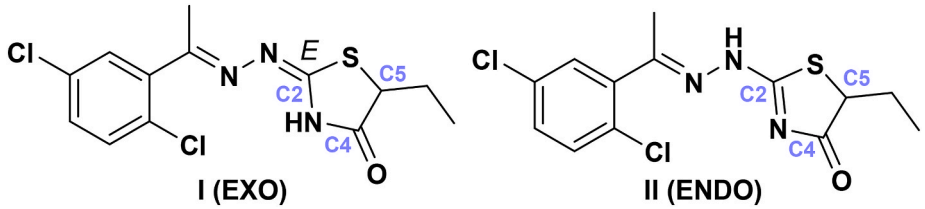

Fig. 3. Example of the C═N bond position on the C2 carbon of compound **1c**.

Table 1
Anti-*T. cruzi* activity of thiazolidinones (**1a-3e**).

Compd.	R_1	Cytotoxicity DL_{50} (μM)[a]	Trypomastigotes Y strain *T. cruzi* IC_{50} (μM)[b]	Epimastigotes [DM28c] IC_{50} (μM)[c]
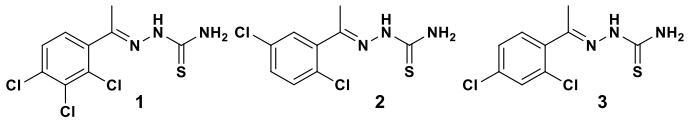				
1	–	84.76	41.80	29.02
2	–	38.32	2.97	6.6
3	–	3.83	3.66	24.79
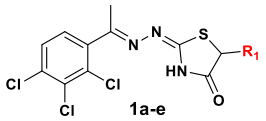				
1a	H	74.64	9.20	66.66
1b	CH_3	71.64	65.47	ND
1c	CH_2CH_3	68.88	34.14	7.16
1d	$CH(CH_3)_2$	>265.26	24.21	47.12
1e	C_6H_5	24.33	30.14	1.96
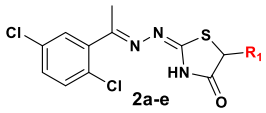				
2a	H	83.06	78.49	ND
2b	CH_3	79.37	41.50	60.33
2c	CH_2CH_3	151.97	4.99	58.74
2d	$CH(CH_3)_2$	145.76	57.83	ND
2e	C_6H_5	13.26	0.84	36.21
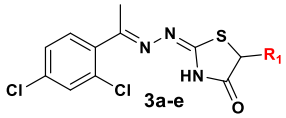				
3a	H	83.06	1.12	ND
3b	CH_3	79.37	7.14	60.33
3c	CH_2CH_3	30.39	2.57	3.42
3d	$CH(CH_3)_2$	29.15	ND	3.45
3e	C_6H_5	132.62	67.35	6.63
BDZ	–	96.06	6.26	6.26
NFX	–	3.48	2.64	ND

ND = Not determined.

[a] Cytotoxic concentration for 50% of mouse splenocytes culture after 24h incubation in the presence of the compounds.

[b] Determined 24 h after incubation of the trypomastigote forms with the compounds. IC_{50} was calculated from five concentrations; IC_{50} values were calculated using at least seven data point points using non-linear regression.

[c] Determined 24 h after incubation of the epimastigote forms with the compounds. IC_{50} was calculated from five concentrations; IC_{50} values were calculated using at least seven data-points using non-linear regression. BDZ: Benznidazole. NFX: Nifurtimox.

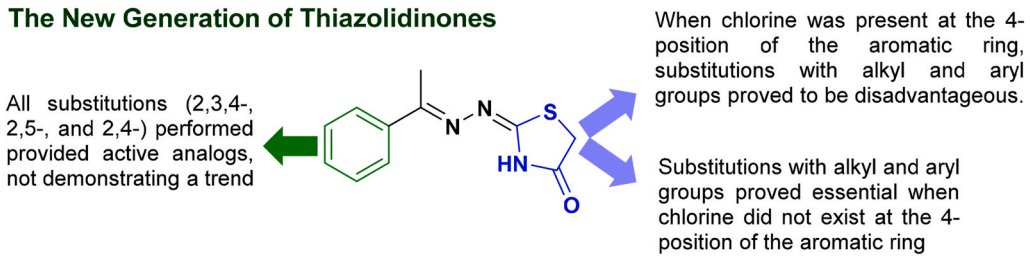

Fig. 4. Summary of the biological structure-activity relationships of the new generation of thiazolidinones.

heterocycle benefited the trypanocidal activity [13,23].

For sub-series (**3a-e**), it was observed that the analogs **3b** (IC_{50} = 7.14 μM) and **3c** (IC_{50} = 2.57 μM) showed promising activity. They present a methyl and ethyl group, respectively, at the C5 position of the thiazolidinone ring. Although, compound **3a** (IC_{50} = 1.12 μM), which is the most active analog of this sub-series, does not show substitution at the C5 position of the heterocyclic ring, which leads us to suggest that if the 4-position of the aromatic ring is substituted with chlorine, the

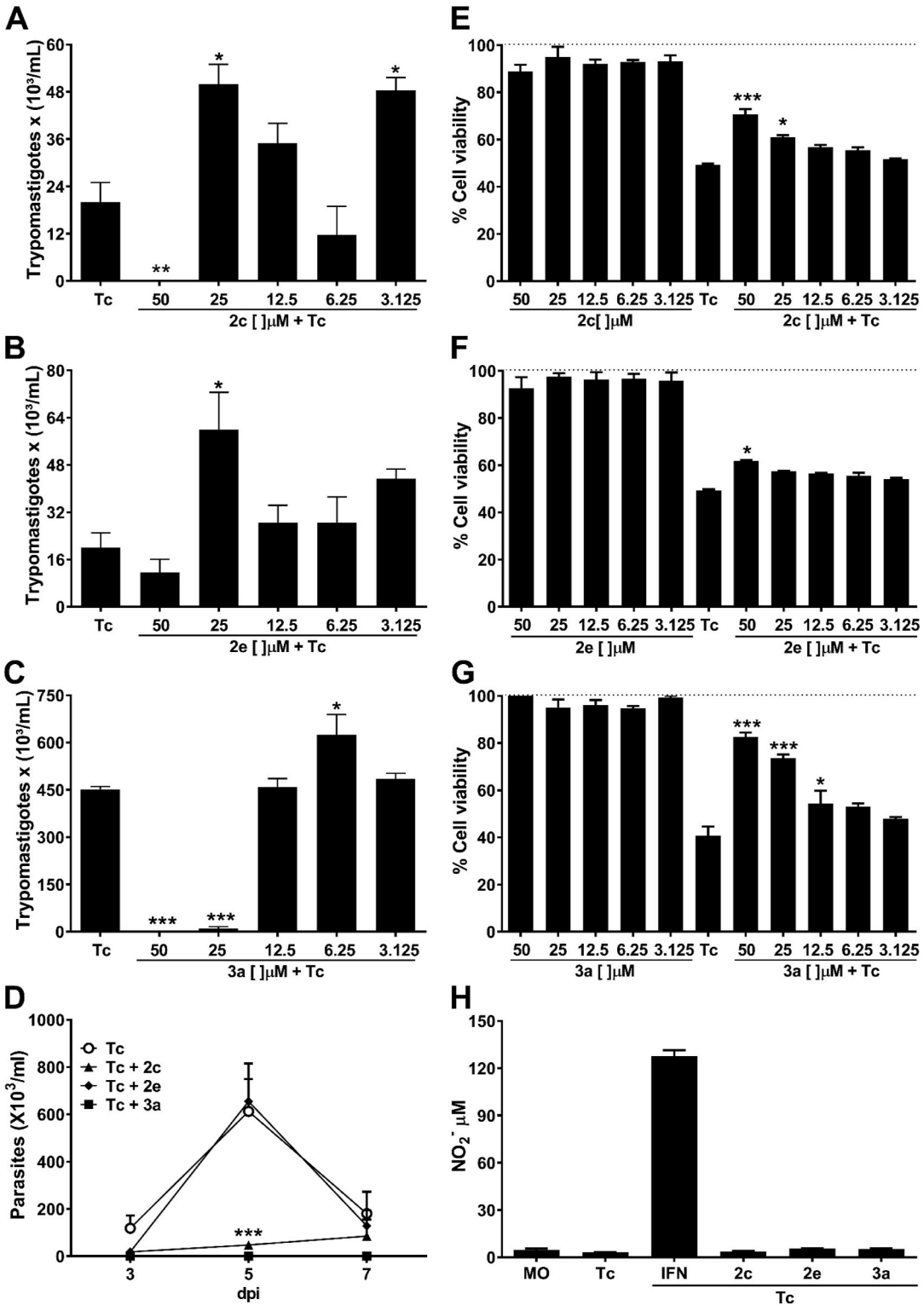

Fig. 5. Potent trypanocidal activity of **2c** and **3a** on macrophages. Peritoneal macrophages of C57BL/6 mice were cultured and infected with *T. cruzi* trypomastigote forms at the ratio of 5: 1 (parasite/cell) and stimulated or not, with IFN-ɣ (100 ng/ml) or **2c**, **2e**, **3a** (3.125, 6.25, 12.5, 25 and 50 μM). Parasite growth was measured by counting trypomastigote forms released in the supernatant at different times after infection (**A-D** = dose-response and D = 50 mM). Cell damage was evaluated by measuring MTT cytotoxicity assay after 7 days of treatments with different 2c, 2e, and 3a (E–G) concentrations. Nitric Oxide was measured by Griess method in the culture supernatant after 72 h of stimulation with **2c**, **2e**, **3a** at the concentration of 50 mM. Data expressed as a mean ± SEM – Two-way ANOVA, post-test Bonferroni; One-way ANOVA, post-test Tukey: ***$p < 0.001$, **$p < 0.01$, *$p < 0.05$.

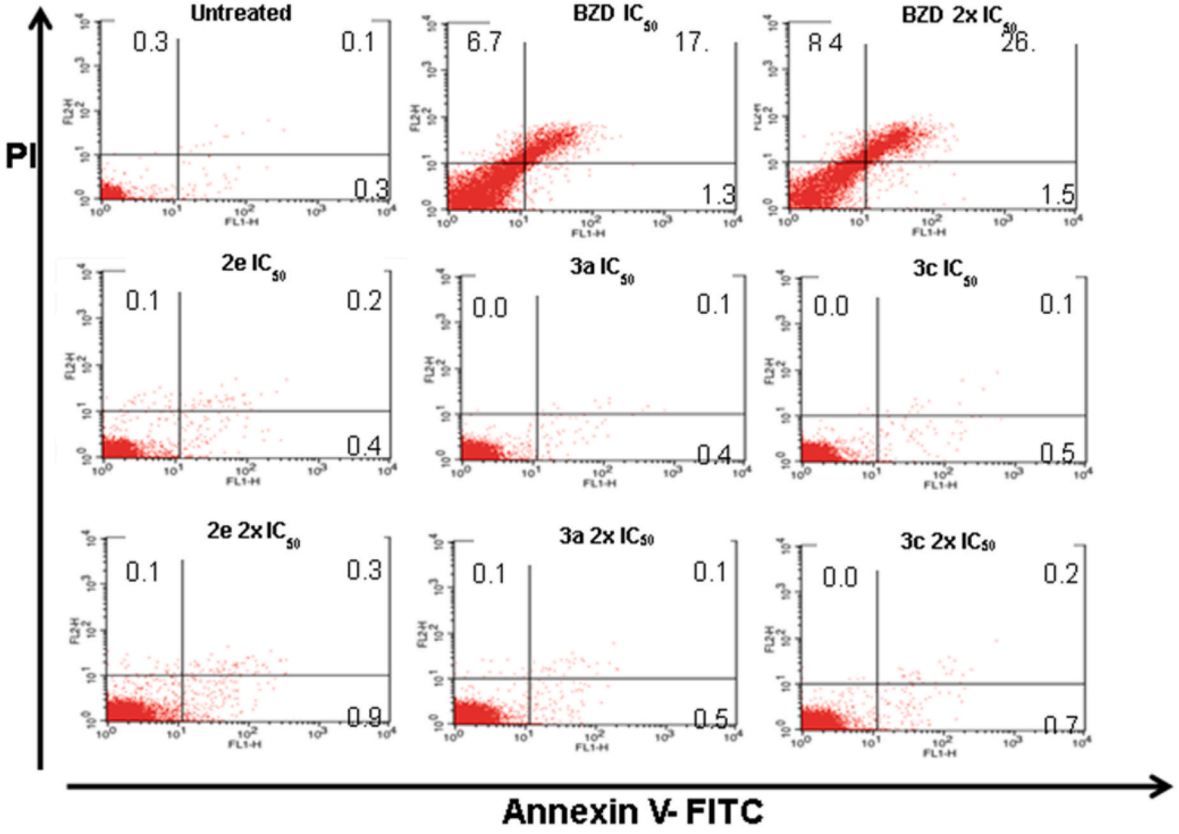

Fig. 6. Flow cytometry analysis for trypomastigote form of *T. cruzi.* Parasites were examined by flow cytometry with annexin V and PI staining. The percentage of cells in each quadrant represents: lower left, double negative; upper left, PI single positive; lower right, annexin V single positive; upper right, PI and annexin V double positive.

substitution at the C5 position of the heterocyclic becomes disadvantageous. Fig. 4 shows a summary of the biological structure-activity relationships.

Compounds **1a** (IC_{50} = 9.20 μM), **2c** (IC_{50} = 4.99 μM) and **3b** (IC_{50} = 7.14 μM) were equipotent to Benznidazole (IC_{50} = 6.26 μM), while compounds **2e** (IC_{50} = 0.84 μM), **3c** (IC_{50} = 2.57 μM) and **3a** (IC_{50} = 1.12 μM) demonstrated greater activity than Benznidazole (IC_{50} = 6.26 μM). A highlight must be made for compound **3a** (IC_{50} = 1.12 μM), which has a selectivity index of 74.16, five times that of Benznidazole (IS = 15.34). The compounds were also tested against the epimastigote form of *T. cruzi*, but the results obtained did not present a significant correlation with the data obtained on trypomastigotes.

3.4. Macrophage culture, T. cruzi infection, MTT and nitric oxide evaluation

Macrophages are innate immune cells that play an essential role in controlling the replication of parasites and stimulating adaptive immunity cells. In peritoneal macrophages submitted to *T. cruzi* infection and treated with **2c** and **3a**, but not with **2e**, in a dose-response curve (Fig. 5A–C), it was possible to reduce the release of trypomastigote forms relative to their control 5 days after infection at the concentration of 50 μM of the **2c** and 50 and 25 μM of the **3a** (Fig. 5A, **C,** and **5D**). In the cell viability test measured by the MTT cytotoxicity assay, all the concentrations of **2c**, **2e,** and **3a** tested showed no cytotoxic activity on macrophages (Fig. 5E–G). Moreover, *T. cruzi*-infected macrophages stimulated with the concentrations of **2c** (50 and 25 μM), **2e** (50 μM), or **3a** (50, 25, and 12.5 μM), presented higher viability when compared with unstimulated infected macrophages (Fig. 5D, E, and 5F). It is worth mentioning that, among the tested compounds, the **3a** at 50 μM presented higher trypanocidal activity associated (Fig. 5D) with lower cellular toxicity (Fig. 5G).

Altogether, these results suggested that **2c** and **3a** can control the release of *T. cruzi* by macrophages *in vitro*. The increased trypanocidal activity induced by **2c** and **3a** was not related to increased nitric oxide production since NO levels were increased only in the presence of IFN-γ (Fig. 5H). This indicates that the trypanocidal activity of **2c** and **3a** is independent of NO release.

3.5. Flow cytometry analysis for trypomastigote form of T. cruzi

The flow cytometry analysis was released to compounds **2e**, **3a,** and **3c** by using IC_{50} and twice IC_{50} values. It was observed that compound **2e** (IC_{50} and 2x IC_{50}) induced significantly labeling compatible with necrosis and apoptosis in trypomastigotes. Similar results were found in parasites treated with BDZ, the reference drug, and positive control used in this assay (Fig. 6).

3.6. Ultrastructural studies of T. cruzi

In order to investigate the effects of 4-thiazolidinones chlorine derivatives on parasite morphology, the most active compounds of this work were selected. Analysis by scanning electron microscopy showed that *Trypanosoma cruzi* trypomastigote forms of the control group

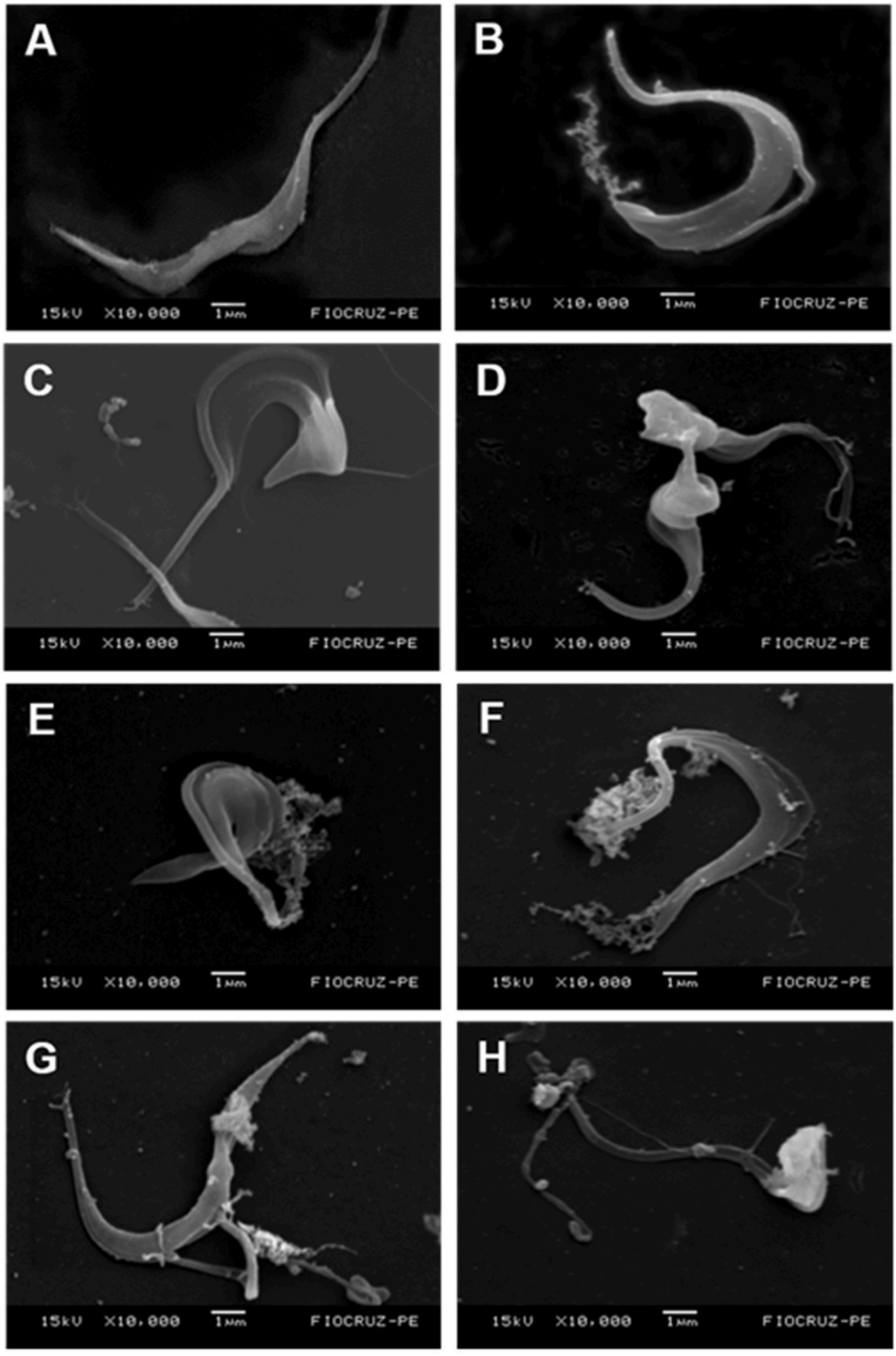

Fig. 7. (A–H). Electron micrographs of *Trypanosoma cruzi* trypomastigote forms.

(Fig. 7A) showed typical morphology with long flagella and preserved body topography. The cells treated with BDZ (Fig. 7B) presented a shortening of the flagellum, curvature of the body with extravasation of the internal content. The cells treated with the compounds **2e** (Fig. 7C and **D**), **3a** (Fig. 7E and **F**), and **3c** (Fig. 7G and **H**) presented morphological alterations such as flagellum shortening, retraction, and curvature of the parasite body and extravasation of the internal content.

In the present study, the activity of this compound (**2e, 3a** and **3c**)

Table 2
Physicochemical property profile of thiazolidinone derivatives, calculated by online software SwissADME (http://www.swissadme.ch/index.php).

CPD.	MW < 500	MLog P <=4.15	H-bond donors <5	H-bond acceptors <10	Lipinski violations	#Rotable bonds <10	TPSA <=140
1	296.6	3.1	2	1	0	3	82.5
2	262.16	2.55	2	1	0	3	82.5
3	262.16	2.55	2	1	0	3	82.5
1a	336.62	3.12	1	3	0	2	79.12
1b	350.65	3.38	1	3	0	2	79.12
1c	364.68	3.63	1	3	0	3	79.12
1d	378.7	3.87	1	3	0	3	79.12
1e	412.72	4.34	1	3	1	3	79.12
2a	302.18	2.59	1	3	0	2	79.12
2b	316.21	2.86	1	3	0	2	79.12
2c	330.23	3.11	1	3	0	3	79.12
2d	344.26	3.36	1	3	0	3	79.12
2e	378.28	3.84	1	3	0	3	79.12
3a	302.18	2.59	1	3	0	2	79.12
3b	316.21	2.86	1	3	0	2	79.12
3c	330.23	3.11	1	3	0	3	79.12
3d	344.26	3.36	1	3	0	3	79.12
3e	378.28	3.84	1	3	0	3	79.12

Table 3
ADME properties of most active compounds.

Compound	[a]BBB permeant	[b]GI absorption	Bioavailability Score
2c	No	High	55
2e	No	High	55
3a	No	High	55
BDZ	No	High	55

[a] BBB - blood-brain barrier.

[b] GI - Gastrointestinal absorption.

can be observed through ultrastructural changes caused in *Trypanosoma cruzi*, which certainly makes the cell unfeasible.

3.7. Physicochemical properties

To better understand the physicochemical contributions of the synthesized compounds, the online software SwissADME [24] (http://www.swissadme.ch/index.php) was used to determine the physicochemical descriptors and define the pharmacokinetic properties and drug-like nature of all compounds. Physicochemical properties were important to determine if they agree with Lipinski's rule [25,26]. Compounds following at least three of the four criteria are considered to respect the Lipinski Rule [26]. As we can see in Table 2, all synthesized compounds are compatible with the Lipinski Rule. Another attractive property is the number of rotatable bonds and the topological polar surface area (TPSA). A large number of rotatable bonds ($\geq$10) have been associated with poor oral bioavailability [26]. Compounds with a low TPSA ($\leq$140 Å^2) tend to have higher oral bioavailability [27,28]. All synthesized compounds present appropriate TPSA and number of rotatable bonds, agreeing with the Veber rule.

As demonstrated in Table 3, the most active compounds shown variable permeability based on gastrointestinal absorption (GI), according to the BOILED-Egg predictive model (Brain Or IntestinaL EstimateD permeation method). The toxicity result of the drug from SwissADME shows it to be very soluble in the body, it also has a high Gastrointestinal Tract (GI) absorption, and the drug was not blood-brain barrier permeant. These are important as they would allow the drug to have high uptake. The most selective derivatives showed high gastrointestinal absorption (**2c**, **2e,** and **3a**). Concerning oral bioavailability, it has expected 0.55 of the probability of oral bioavailability score >10% in the rate for all compounds, similar to Benznidazole. All these data suggest a good in silico drug-likeness profile and exceptional chemical stabilities for all compounds synthesized.

4. Conclusion

Three thiosemicarbazones (**1**–**3**) and fifteen thiazolidinones derivatives (**1a-e**, **2a-e**, **3a-e**), based on the bioisosteric strategy, were obtained reasonable yields using a simple methodology. The new generation of 4-thiazolidinones presents a thiazolidinone heterocycle, a di or tri-chlorophenyl-ethylidenehydrazone, and H or alkyl substituents in the C5 position of thiazolidinone ring. Concerning cytotoxicity in mouse splenocytes, in general, cyclization is beneficial since cyclic compounds presented better toxicity indices when compared to their non-cyclic bioisosteres. The *in vitro* anti-*T. cruzi* activity against trypomastigotes of Y strain revealed that between all series, compounds **1a**, **2c** and **3b** were equipotent to Benznidazole, while compounds **2e**, **3a**, and **3c** demonstrated higher activity than Benznidazole, with compound **3a** (IC_{50} = 1.12 μM) having a selectivity index of 74.16, five times that of Benznidazole (IS = 15.34). In peritoneal macrophages submitted to *T. cruzi* infection **2c** and **3a**, it was possible to reduce the release of trypomastigote forms relative to their control 5 days after infection. When *T. cruzi*-infected macrophages stimulated with **2c**, **2e**, **3a** exhibited higher viability when compared with unstimulated infected macrophages. Parasites treated with the compounds **2e**, **3a** and **3c** presented flagellum shortening, retraction and curvature of the parasite body, and extravasation of the internal content. All synthesized compounds are compatible with the Lipinski and Veber rules.

Declaration of competing interest

The authors declare that they have no known competing financial interests or personal relationships that could have appeared to influence the work reported in this paper.

Acknowledgment

This work was funded by Conselho Nacional de Desenvolvimento Científico e Tecnológico (CNPq) and Fundação de Amparo à Ciência e Tecnologia de Pernambuco (FACEPE). A.C.L.L. is receiving a CNPq senior fellowship. G.B.O.F. received a FACEPE PhD scholarship. M.V.O.C. is thankful to CNPq (427078/2016–4) and FACEPE (APQ-0350-4.03/18) for financial support. The authors are thankful to the Departamento de Química Fundamental (DQF-UFPE) for recording the ^{1}H NMR, ^{13}C NMR, and IR spectra of compounds. We are also thankful to Centro de Tecnologias Estratégicas do Nordeste (CETENE) for recording the MS spectra of compounds. All authors declare no competing financial interest.

Appendix A. Supplementary data

Supplementary data to this article can be found online at https://doi.org/10.1016/j.cbi.2021.109514.

References

[1] WHO | what Is Chagas Disease, WHO, 2016.
[2] J.C.P. Dias, M.A.S. Coura JR., Yasuda the present situation, challenges, and perspectives regarding the production and utilization of effective drugs against human Chagas disease, Rev. Soc. Bras. Med. Trop. 47 (2014) 123–125.
[3] WHO | Transmission of Chagas Disease, WHO, 2016.
[4] N. Klein, I. Hurwitz, R. Durvasula Globalization of Chagas Disease, A growing concern in non-endemic countries, Epidemiol. Res. Int. 2012 (2012) 1–13.
[5] J.P.P. Dias, Human Chagas disease and migration in the context of globalization: some particular aspects, J. Trop. Med. 2013 (2013) 1–9.
[6] J.M. Kraus, C.L.M.J. Verlinde, M. Karimi, G.I. Lepesheva, M.H. Gelb Buckner Fs, Rational modification of a candidate cancer drug for use against Chagas disease, J. Med. Chem. 52 (6) (2009) 1639–1647.
[7] E. Chatelain, Chagas disease drug discovery: toward a new era, J. Biomol. Screen. [Internet] 20 (1) (2015) 22–35.
[8] J.M. Kraus, H.B. Tatipaka, S.A. McGuffin, et al., Second generation analogues of the cancer drug clinical candidate tipifarnib for anti-chagas disease drug discovery, J. Med. Chem. 53 (10) (2010) 3887–3898.
[9] A.F. Francisco, S. Jayawardhana, M.D. Lewis, M.C. Taylor, J.M. Kelly, Biological factors that impinge on Chagas disease drug development, Parasitology 144 (14) (2017) 1871–1880.
[10] C.B. Scarim, D.H. Jornada, R.C. Chelucci, L. Almeida, J.L. Santos, M.C. Chung, Current advances in drug discovery for Chagas disease, Eur. J. Med. Chem. 155 (2018) 824–838.
[11] G.B. Oliveira Filho, M.V.O. Cardoso, J.W.P. Espíndola, et al., Structural design, synthesis and pharmacological evaluation of thiazoles against Trypanosoma cruzi, Eur. J. Med. Chem. 141 (2017) 346–361.
[12] J.W.P. Espíndola, M.V.O. Cardoso, G.B. Oliveira Filho, et al., Synthesis and structure–activity relationship study of a new series of antiparasitic aryloxyl thiosemicarbazones inhibiting Trypanosoma cruzi cruzain, Eur. J. Med. Chem. 101 (2015) 818–835.
[13] G.B. Oliveira Filho, M.V.O. Cardoso, J.W.P. Espíndola, et al., Structural design, synthesis and pharmacological evaluation of 4-thiazolidinones against Trypanosoma cruzi, Bioorg. Med. Chem. 23 (2015) 7478–7486.
[14] L.B. Costa, M.V.O. Cardoso, G.B. Oliveira Filho, et al., Compound profiling and 3D-QSAR studies of hydrazone derivatives with activity against intracellular Trypanosoma cruzi, Bioorg. Med. Chem. 24 (8) (2016) 1608–1618.
[15] M.V.O. Cardoso, L.R.P. Siqueira, E.B. Silva, et al., 2-Pyridyl thiazoles as novel anti-Trypanosoma cruzi agents : structural design , synthesis and pharmacological evaluation, Eur. J. Med. Chem. 86 (9) (2014) 48–59.
[16] P.A.T.M. Moraes, P.A.T. Gomes, M.O. Barbosa, E.F. Santiago, et al., New 1,3-thiazole derivatives and their biological and ultrastructural effects on Trypanosoma cruzi, Eur. J. Med. Chem. 121 (2016) 387–398.
[17] D.R.M. Moreira, A.D.T. Oliveira, P.A.T.M. Gomes, et al., Conformational restriction of aryl thiosemicarbazones produces potent and selective anti-Trypanosoma cruzi compounds which induce apoptotic parasite death, Eur. J. Med. Chem. 75 (2014) 467–478.
[18] D.R.M. Moreira, A.C.L. Leite, M.V.O. Cardoso, et al., Structural design, synthesis and structure-activity relationships of thiazolidinones with enhanced anti-trypanosoma cruzi activity, ChemMedChem 9 (1) (2014) 177–188.
[19] D.R.M. Moreira, S.P.M. Costa, M.Z. Hernandes, et al., Structural investigation of anti-Trypanosoma cruzi 2-iminothiazolidin-4-ones allows the identification of agents with efficacy in infected mice, J. Med. Chem. 55 (24) (2012) 10918–10936.
[20] X. Du, C. Guo, E. Hansell, et al., Synthesis and Structure−Activity relationship study of potent trypanocidal thio semicarbazone inhibitors of the trypanosomal cysteine protease cruzain, J. Med. Chem. 45 (13) (2002) 2695–2707.
[21] M.Z. Hernandes, M.M. Rabello, A.C.L. Leite, et al., Studies toward the structural optimization of novel thiazolylhydrazone-based potent antitrypanosomal agents, Bioorg. Med. Chem. 18 (22) (2010) 7826–7835.
[22] C.P. Kaushik, Ashima Pahwa. Convenient synthesis, antimalarial and antimicrobial potential of thioethereal 1,4-disubstituted 1,2,3-triazoles with ester functionality, Med. Chem. Res. 27 (2018) 458–469.
[23] D.R.M. Moreira, S.P.M. Costa, M.Z. Hernandes, et al., Structural investigation of anti-trypanosoma cruzi 2-iminothiazolidin-4- ones allows the identification of agents with efficacy in infected mice, J. Med. Chem. 55 (24) (2012).
[24] Daina1 Antoine, Olivier Michielin, Vincent Zoete, SwissADME: a free web tool to evaluate pharmacokinetics, druglikeness and medicinal chemistry. friendliness of small molecules, Sci. Rep. 7 (4) (2017) 1–13.
[25] C.A.L. Ã, Lead Profiling Lead- and Drug-like Compounds : the Rule-Of-Five Revolution, 2004, pp. 337–341.
[26] I. Franc, A. Lipinski, P.J. Feeney, et al., Experimental and computational approaches to estimate solubility and permeability in drug discovery and development settings, Adv. Drug Deliv. Rev. 23 (1–3) (1997) 3–25.
[27] D.F. Veber, S.R. Johnson, H.-Y. Cheng, B.R. Smith, K.W. Ward, K.D. Kopple, Molecular properties that influence the oral bioavailability of drug candidates, J. Med. Chem. 45 (12) (2002) 2615–2623.
[28] N.A. Meanwell, Improving drug candidates by design: a focus on physicochemical properties as a means of improving compound disposition and safety, Chem. Res. Toxicol. 24 (9) (2011) 1420–1456.